Available online at www.sciencedirect.com
SCIENCE DIRECT
ELSEVIER
Coordination Chemistry Reviews 250 (2006) 1562–1579
COORDINATION CHEMISTRY REVIEWS
www.elsevier.com/locate/ccr

Review

High sensitivity lanthanide(III) based probes for MR-medical imaging

S. Aime [a,*], S. Geninatti Crich [a], E. Gianolio [a], G.B. Giovenzana [b], L. Tei [a], E. Terreno [a]

[a] *Università di Torino, Dip. Chimica IFM,Via P. Giuria 7, 10125 Torino, Italy*
[b] *DiSCAFF, Università del Piemonte Orientale, "A. Avogadro", Via Bovio 6, 28100 Novara, Italy*

Received 1 December 2005; accepted 7 March 2006
Available online 27 March 2006

Contents

Abstract

To date, Gd(III) based contrast agents are commonly used in MR-medical imaging. In the last 15 years, our overall goal has been to develop targeting and responsive Gd(III) containing probes for innovative magnetic resonance imaging (MRI) applications. Understanding the relationships between structure and dynamics of lanthanide(III) chelates has been fundamental for the development of high sensitive Gd(III) based agents. Moreover, the observed relaxivity may act as a reporter of a specific parameter of the microenvironment in which the contrast agent distributes by using properly designed systems in which one structural or motional parameter is affected by the parameter of interest.

From targeting human serum albumin for the development of angiographic agents, our research efforts are now addressing the visualization of molecules (characterizing diseased states) that are present at much lower concentration. By different routes, it has become possible to visualize, in an MR image, cells that have been labeled with Gd(III) chelates.

Finally, the shift properties of paramagnetic lanthanide(III) complexes (Ln ≠ Gd) have been exploited for designing a novel class of contrast agents based on the transfer of saturated magnetization to the bulk water signal from exchangeable protons on the contrast agent molecules (chemical exchange saturation transfer (CEST) agents) or from water molecules interacting with a lanthanide shift reagent.

Keywords: Paramagnetic lanthanide(III) complexes; MRI contrast agents; Gd-complexes; CEST agents; Targeting agents; Responsive agents

* Corresponding author. Tel.: +39 011 6707520; fax: +39 011 6707855.
E-mail address: silvio.aime@unito.it (S. Aime).

0010-8545/$ – see front matter © 2006 Elsevier B.V. All rights reserved.
doi:10.1016/j.ccr.2006.03.015

1. Introduction

The superb spatial resolution and the outstanding capacity of differentiating soft tissues have determined the widespread success of magnetic resonance imaging (MRI) in clinical diagnosis [1,2]. The contrast in an MR image is the result of a complex interplay of numerous factors, including the relative T_1 and T_2 relaxation times, proton density of the imaged tissues and instrumental parameters.

The MR image contrast can be further enhanced by administration of suitable MRI contrast agents (CA). In fact, it was shown that CA causes a dramatic variation of the water proton relaxation rates, thus providing physiological information beyond the impressive anatomical resolution commonly obtained in the uncontrasted images. CA are widely used clinically to assess organ perfusion, disruption of the blood–brain barrier, occurrence of abnormalities in kidney clearance, and circulation issues.

Several other applications, primarily in the field of tumor targeting, are currently under advanced development with the promise of soon being available in clinical practice. Nowadays, about 35% of the MRI examinations make use of CA, but this percentage is predicted to increase further following the development of more effective and specific contrast media than those currently available.

Unlike contrast agents used in X-ray computed tomography and in nuclear medicine, MRI contrast agents are not directly visualized in the image. Only their effects are observed: contrast is affected by the variation that the CA causes on water protons relaxation times, and consequently on the intensity of the NMR signal [3,4]. Generally, the purpose of a CA is to reduce T_1 in order to obtain an intense signal in short times and a better signal-to-noise ratio with the acquisition of a higher number of measurements. CAs that predominantly reduce T_1 are called *positive*, whereas those that only largely affect T_2 are called *negative*. Since unpaired electrons are able to remarkably reduce T_1 and T_2, the search for positive CAs has been mainly oriented towards paramagnetic metal complexes. The paramagnetic metal ions most extensively studied are either transition metals or in the lanthanide series.

As far as lanthanides are concerned [5], the attention has been essentially focused on Gd(III) both for its high paramagnetism (seven unpaired electrons) and for its favourable properties in terms of electronic relaxation [6]. This metal does not possess any known physiological function in mammalians, and its administration as a free ion is strongly toxic even at low doses (10–20 $\mu mol\,kg^{-1}$). For this reason, it is necessary to use ligands that form very stable chelates with the lanthanide ion [3,4]. The high affinity shown by Gd(III) towards some polyaminocarboxylic acids, either cyclic or linear, has been exploited to form very stable complexes (up to $\log K_{ML} > 20$). The first CA approved for clinical use was Gd-DTPA (Magnevist®, Schering AG, Germany) that, in more than 10 years of clinical experimentation, has been administered to more than 20 million patients. Other Gd(III) based CA similar to Magnevist® became soon available: Gd-DOTA (Dotarem®, Guerbert SA, France), Gd-DTPA-BMA (Omniscan®, GE Health, USA) and Gd-HPDO3A (Prohance®, Bracco Imaging, Italy) (Fig. 1) [5]. These CA have very similar pharmacokinetic properties because they distribute in the extracellular fluid and are eliminated via glomerular filtration. They are particularly useful to delineate lesions as a result of the disruption of the blood–brain barrier. Two derivatives of Gd-DTPA have been successively introduced, Gd-EOB-DTPA [7] (Eovist®, Schering AG, Germany) and Gd-BOPTA [8] (Multihance®, Bracco Imaging, Italy) (Fig. 1). They are characterized by an increased lipophilicity due to the introduction of an aromatic substituent on the carbon backbone of the DTPA ligand. This modification significantly alters the pharmacokinetics and the biodistribution of these CA as compared to the parent Gd-DTPA.

Paramagnetic chelates of Mn(II) (five unpaired electrons) have also been considered. The main drawback appears to be related to the stability of these complexes. Mn(II) is an essential metal, therefore the evolution has selected biological structures able to sequester Mn(II) ions with high efficiency. Combined with the fact that Mn(II) forms highly labile coordination complexes, it has been difficult to design Mn(II) chelates that maintain their integrity when administered to living organisms. Actually, Mn-DPDP (Fig. 2) has entered the clinical practice and is recommended as a hepatotropic agent [9]. It is the only agent that does its job by releasing metal ions to endogenous macromolecules. The huge proton relaxation enhancement brought about by the resulting Mn(II) protein adduct is responsible for the MRI visualization of hepatocytes also at low administered doses of Mn-DPDP.

Iron(III), having the same number of unpaired electrons as Mn(II), has entered the field of MRI contrast agents in the form of iron oxide particles. Such water insoluble systems yield very strong T_2-effects as the result of a dramatic long-range disturbance in the magnetic field homogeneity. These agents are made of a crystalline core of superparamagnetic iron(III) oxide (SPIO, maghemite and γ-Fe_2O_3) surrounded by coating materials like dextran or carboxydextran. The diameter of the iron oxide core is just 3–5 nm whereas the overall particle may range from few tens to few hundreds of nanometres in size [10,11]. These agents provide excellent (negative) contrast when administered at iron doses as low as 8–15 $\mu mol\,kg^{-1}$ body weight. Once administered intravenously, as particles, these agents accumulate in the cells of the reticuloendothelial system. The pharmacodynamic properties of the iron oxide particles are affected by either the size or the overall electric charge. The smaller particles remain in the blood circuit for a time long enough to be considered as blood pool agents for angiographic assays.

The field of medical imaging is rapidly evolving towards the development of molecular imaging procedures aimed at visualizing molecular events occurring at cellular levels. This would represent a breakthrough in clinical settings as, in addition to provide early diagnosis, it would allow the assessment of an underlying therapy by visualizing specific molecules and biomarkers that are the "signature" of the pathology. Such approach will be highly beneficial in ensuring the patient that the chosen therapy is going to provide the expected effects, as it will largely anticipate the time currently required for assessment based on anatomical changes.

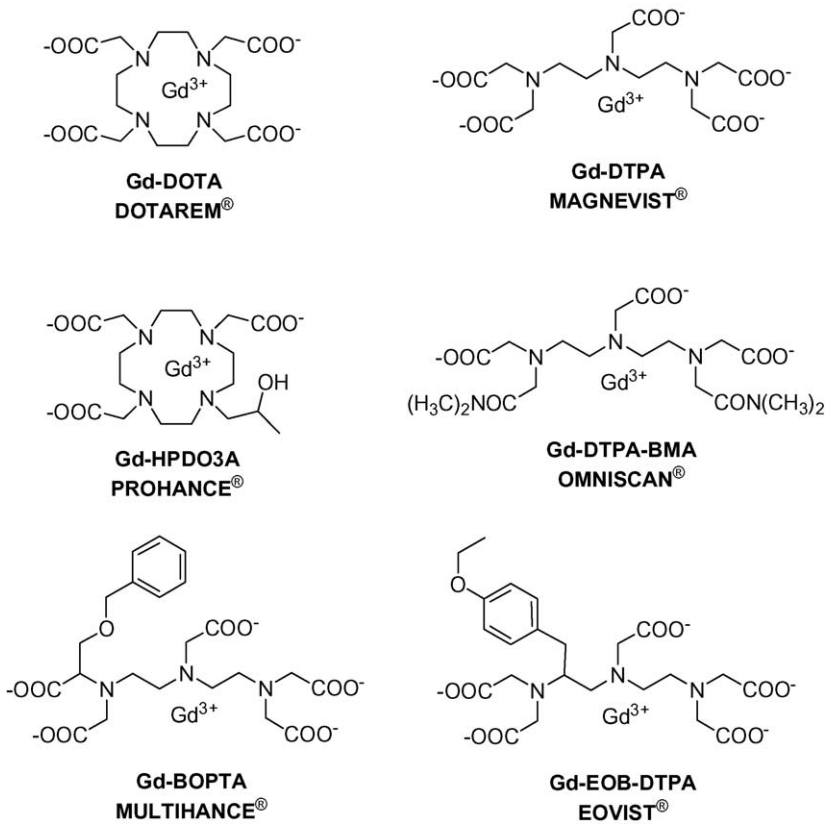

Fig. 1. Structures of the Gd(III) based MRI contrast agents currently used in the clinical practice.

The need of targeting molecules that are present at very low concentration requires the development of a novel class of CAs characterized by higher contrasting ability and improved targeting capabilities. In this survey we intend to tackle some basic issues that are highly relevant to the use of Gd(III) based systems in molecular imaging applications, namely: (1) how to achieve very high relaxivities for Gd(III) complexes on the basis of the current understanding of the determinants of the "relaxivity parameter"; (2) how one may envisage efficient routes for the delivery of a high number of Gd(III) complexes at the site of interest; (3) the most practical ways to pursue the cell-internalization of a high number of Gd(III) complexes.

Finally, a new class of MRI contrast agents, the so-called chemical exchange saturation transfer (CEST) agents, will be discussed. These systems contain at least one pool of exchangeable protons which, upon irradiating at their absorption frequency, transfer saturated magnetization to the bulk water signal. The use of lanthanide or transition metal paramagnetic chelates (PARACEST agents) has been shown to be particularly beneficial because the paramagnetic ion induces a large shift of resonance on the nuclei surrounding it. The peculiar properties of PARACEST agents allow to tackle applications that are not possible with the relaxation enhancement agents.

Fig. 2. Structure of Mn-DPDP, a manganese(II) based MRI contrast agent used in the clinical practice.

2. Determinants of relaxivity

First of all, to be considered as a potential CA, a Gd-complex must have a high thermodynamic and, possibly, kinetic inertness, and should have at least one water molecule coordinated to the metal ion in fast exchange with the bulk water. In fact, it is the exchange with the solvent water molecules that allows to affect the relaxation process of all protons present in the region in which the CA distributes. The Gd(III) chelate efficiency is commonly evaluated in vitro by the measure of its relaxivity (r_1), that, for commercial CAs as Magnevist, Dotarem, Prohance and Omniscan, is around 3.4–3.5 $mM^{-1}\,s^{-1}$ (at 20 MHz and 39 °C). The observed longitudinal relaxation rate (R_1^{obs}) of the water protons in an aqueous solution containing the paramagnetic complex is the sum of three contributions (Eq. (1)) [12]: (i) the diamagnetic one, whose value corresponds to proton relaxation rate measured in the presence of a diamagnetic (La, Lu, Y) complex of the same ligand; (ii) the paramagnetic one, relative to the exchange of water molecules from the inner coordination sphere of the metal ion with bulk water (R_{1p}^{is}); (iii) the param-

agnetic one relative to the contribution of water molecules that diffuse in the outer coordination sphere of the paramagnetic center (R_{1p}^{os}). Sometimes, also a fourth paramagnetic contribution is taken in account, that is due to the presence of mobile protons or water molecules (normally bound to the chelate through hydrogen bonds) in the second coordination sphere of the metal [13]:

$$R_1^{obs} = R_1^{o} + R_{1p}^{is} + R_{1p}^{os} \quad (1)$$

The inner sphere contribution is directly proportional to the molar concentration of the paramagnetic complex, to the number of water molecules coordinated to the paramagnetic center, q, and inversely proportional to the sum of the mean residence lifetime, τ_M, of the coordinated water protons and their relaxation time, T_{1M} (Eq. (2)):

$$R_{1p}^{is} = \frac{q[C]}{55.5(T_{1M} + \tau_M)} \quad (2)$$

The latter parameter is directly proportional to the sixth power of the distance between the metal center and the coordinated water protons (r) and depends from the molecular reorientational time, τ_R, of the chelate, from the electronic relaxation times, T_{iE} ($i = 1, 2$), of the unpaired electrons of the metal (which depend on the applied magnetic field strength) and from the applied magnetic field strength itself (Eqs. (3) and (4)):

$$\frac{1}{T_{1M}} = \frac{2}{15}\left(\frac{\mu_0}{4\pi}\right)^2 \frac{\gamma_I^2 g_e^2 \mu_B^2 S(S+1)}{r_H^6}\left(\frac{7\tau_c}{1+\omega_S^2\tau_c^2} + \frac{3\tau_c}{1+\omega_I^2\tau_c^2}\right) \quad (3)$$

$$\tau_c^{-1} = \tau_R^{-1} + \tau_M^{-1} + T_{iE}^{-1} \quad (4)$$

The outer sphere contribution depends on T_{iE}, on the distance of maximum approach between the solvent and the paramagnetic solute, on the relative diffusion coefficients and again on the magnetic field strength [14]. The dependence of R_{1p}^{is} and R_{1p}^{os} on magnetic field is very important because the analysis of the magnetic field dependence allows the determination of the principal parameters characterizing the relaxivity of a Gd(III) chelate. This information can be obtained through an NMR instrument in which the magnetic field is changed (Field-Cycling Relaxometer) to obtain the measure of r_1 on a wide range of frequencies (typically 0.01–50 MHz). At the frequencies most commonly used in commercial tomographs (20–63 MHz), τ_R of the chelate is the most important determinant of the observed relaxivity. A quantitative analysis of r_1 dependence on the different structural and dynamic parameters shows that, for systems with long τ_R (e.g. protein bound complex), the maximum attainable r_1 values can be achieved through the optimization of τ_M and T_{iE} [12].

The commercial CA shown in Fig. 1 are monohydrated ($q = 1$) systems with a molecular weight of ca. 600–800 Da that corresponds to rotational correlation times τ_R about 60–80 ps. For this class of polyaminocarboxylate complexes, the exchange lifetime τ_M is typically found to be in the range of few hundreds of nanoseconds and $T_{1E} \approx 1$ ns at 0.5 T and thus the inner sphere relaxivity, r_{ip}^{IS}, assumes a value of ca. 2.5–3.5 $mM^{-1}\,s^{-1}$ at 25 °C. Therefore, as it was early recognized, it is evident that at 0.5 T the overall correlation time is largely dominated by the rotational correlation time, whereas the contribution of both the exchange lifetime and the electronic relaxation play an almost negligible role.

An important structural parameter that influences the *inner sphere* relaxivity is the hydration number q. This represents a scaling factor in the equation that defines inner sphere relaxivity and then a higher number of coordinated water molecules ($q > 1$) provides a clear advantage in terms of efficiency. The use of hepta- or hexadentate ligands would in principle results in Gd(III) complexes with 2- and 3-coordinated water molecules, respectively, but the decrease of the denticity of the ligands is likely to be accompanied by a decrease of their thermodynamic stability and an increase of their toxicity. Furthermore, systems with $q = 2$ may suffer a "quenching" effect upon interacting with endogeneous anions or with proteins, as donor atoms from lactate or Asp or Glu residues may replace the coordinated water molecules [15].

However, some stable Gd(III) chelates containing two *inner sphere* water molecules have been identified and are currently under intense scrutiny. Among them, an interesting class is represented by Gd-HOPO complexes developed by Raymond and co-workers. HOPO ligands [16,17] (Fig. 3) are based on 4-carboxyamido-3,2-hydroxypyridinone chelating units and act as heptadentate ligands towards Gd(III) thus leaving two water molecules in the inner coordination sphere. The peculiar coordinating geometry of Gd-HOPO complexes does not allow an easy replacement of the two water molecules by other ligands. Moreover, the exchange rate of the coordinated water molecules is in the range of the optimal values as well as the electronic relax-

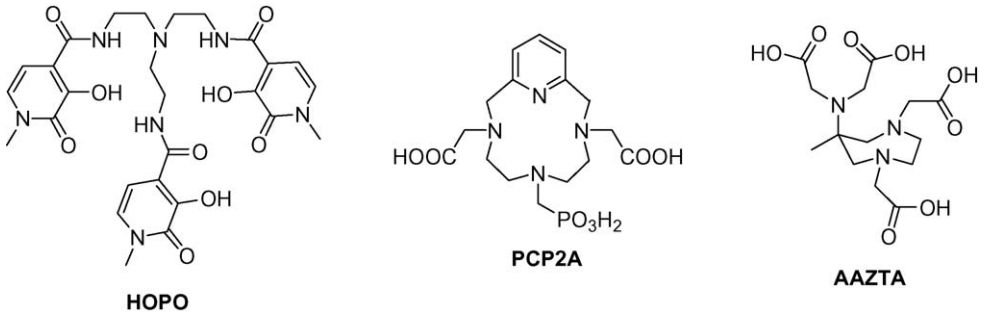

Fig. 3. Schematic representations of three heptadentate ligands.

ation appears to be slow enough to allow the attainment of very high relaxivities [16].

Another system that looks very interesting in this regard is represented by the Gd(III) complex of PCP2A (Fig. 3), a ligand based on a pyridine-containing macrocycle bearing two acetic and one methylenephosphonic arms [17]. Its relaxivity is about two times higher than the values reported for contrast agents currently used in clinical practice. This is the result of the presence of two water molecules in the inner coordination sphere and a significant contribution from water protons bonded to the phosphonate group.

A novel Gd(III) chelate with the heptadentate AAZTA ligand (AAZTA: 6-amino-6-methylperhydro-1,4-diazepinetetraacetic acid; Fig. 3) has been recently characterized [18]. AAZTA is readily obtained in high yields and its Gd(III) complex displays interesting properties to be considered the prototype of a new class of enhanced MRI agents. It is characterized by a quite high relaxivity value (7.1 $mM^{-1}\,s^{-1}$, 20 MHz and 298 K), a relatively fast exchange rate of the coordinated water molecules ($\tau_M = 90$ ns at 298 K), a high thermodynamic stability in aqueous solution and a nearly complete inertness towards the influence of bidentate endogenous anions.

In vitro relaxometric assays did not show any transmetallation effect when Gd-AAZTA was left in the presence of 10-fold excess of $ZnCl_2$, or $MnCl_2$, or $CaCl_2$ for 2 h.

Lengthening of τ_R for systems with two fast exchanging water molecules is one direction to create high relaxivity agents.

Recently, a novel complex made of a heterotritopic ligand which comprises a 2,2′-bipyridine moiety for specific binding to Fe(II) ions and two polyaminocarboxylate groups for binding to Gd(III) ions has been reported (Fig. 4) [19]. The ligand self-assembles with Fe(II) and Gd(III) into a metallostar $[Fe\{Gd_2L(H_2O)_4\}_3]^{4-}$ structure endowed with high relaxivity ($r_{1p} = 33.6\,mM^{-1}\,s^{-1}$ at 40 MHz and 25 °C). The appropriate choice of the chelating moiety ensures to the complex sufficient thermodynamic stability, a water exchange faster than that of commercial agents and two inner sphere water molecules to double the inner sphere contribution to the relaxivity. This metallostar system is rather small compared to other macromolecular contrast agents, however the concurrent chelation of the multifunctional ligand to Fe(II) and Gd(III) ions forces the rotational correlation time of the Gd(III)-water proton vector to be close to that of the entire assembly. Thus, by strong reduction of the internal flexibility, the advantage of the increased molecular size is maximized. Alternatively, an enhanced control of τ_R can also be obtained in non-metallostar Gd-DOTA-like structures by introducing a bulk substituent on each of the four acetate arms in order to fasten the overall molecular rotation around the Gd-water axis [20].

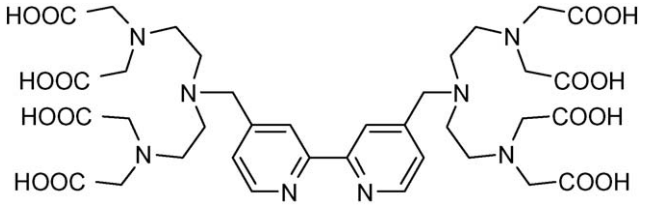

Fig. 4. Schematic representation of a heterotripodic ligand for binding Fe(II) and Gd(III) ions.

As said above, high relaxivities can be attained in the presence of a long reorientational time for the Gd-water proton vector. Basically, two routes have been explored to provide the Gd(III) chelates with long molecular reorientational times: (i) by forming a covalent linkage between the complex and a macromolecular substrate or (ii) by forming a non-covalent adduct between the complex and a slowly tumbling system.

2.1. Adducts with HSA

The latter approach has been widely investigated by using the human serum albumin (HSA) as the interacting substrate. Along this direction, the research activities have been addressed to design Gd(III) chelates bearing on their surface suitable functionalities that promote the reversible binding of HSA [21–23]. Representative examples of such Gd(III) complexes are reported in Fig. 5.

Besides the attainment of high relaxivities (see R_{1p}^{bound} values in Fig. 5), a high binding affinity to HSA enables the Gd(III) chelate to have a long intravascular retention time which is the property required for a good blood pool agent for MR angiography. For the reorientational time of HSA-adducts (ca. 30 ns), the theory of paramagnetic relaxation foresees the attainment of relaxivity values much higher ($r_1 \cong 100\,mM^{-1}\,s^{-1}$) than the values actually obtained. It has been shown that the primary reason for the quenching of the relaxation enhancement is often associated with the occurrence of a relatively long exchange lifetime, τ_M, of the coordinated water [23]. Slow exchange rates of the coordinated water appear to be primarily characteristic of the complex rather than a consequence of the binding to the protein. Thus, for the attainment of high relaxivities one has to avoid Gd(III) chelates displaying slow (i.e. $\tau_M > 500$ ns) exchange rates.

A number of studies have been carried out to elucidate the relationships between the exchange rate of the coordinated water and the structure of the lanthanide(III) complexes [24]. For instance, it has been found that for DOTA and DOTA-like complexes, that exist as a mixture of structural isomers, namely Square AntiPrismatic (SAP) and Twisted Square AntiPrismatic (TSAP) structures, the TSAP isomer displays a much faster water exchange than the SAP isomer (Fig. 6) [25].

In order to get more insight into the problem of why the relaxivity values until now obtained are significantly lower than those predicted by the theory of paramagnetic relaxation, we have recently undertaken a detailed relaxometric study of the interaction of Gd-DOTMA derivatives with HSA [26]. Gd-DOTMA displays a relatively fast exchange of the coordinated molecule likely because it possess a TSAP-like structure. Two new ligands based on DOTMA structure have been synthesized (Fig. 7). ^1H NMR spectra of Eu(III) complexes showed that the TSAP geometry found for the parent DOTMA complexes is maintained. Complex A is soluble enough to allow the determination of the water exchange rate by ^{17}O-T_2 measurements at variable temperature. The obtained value ($\tau_M^{298} = 65$ ns) indicates that the replacement of the methyl with the bulkier biphenyl group does

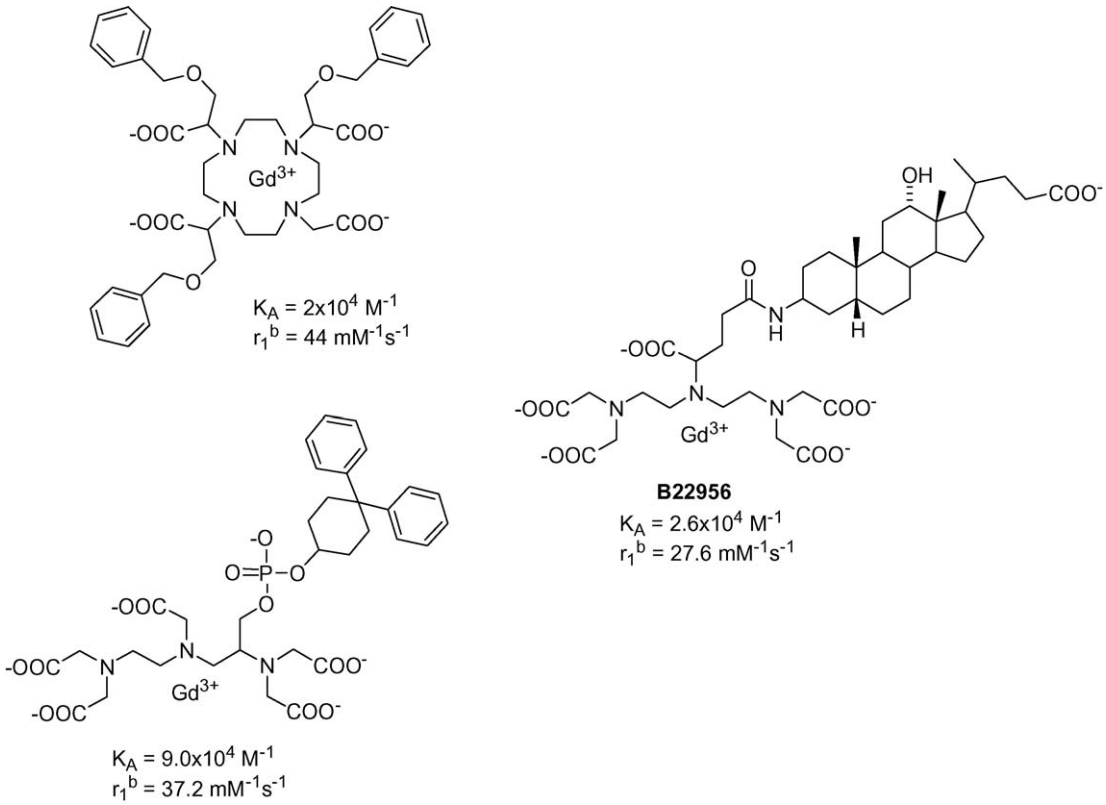

Fig. 5. Structure of three Gd(III) based complexes functionalized with hydrophobic moieties able to promote the interaction with HSA [21,22].

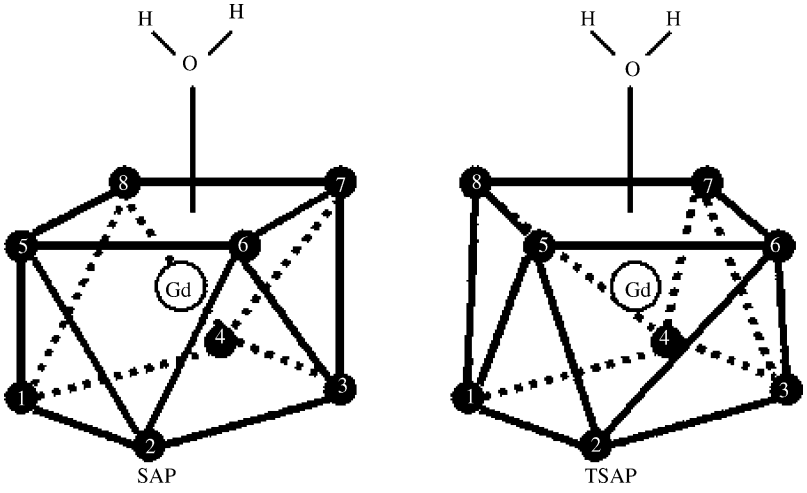

Fig. 6. Structure of the Square AntiPrismatic (SAP) and Twisted Square AntiPrismatic (TSAP) isomers in lanthanide(III) DOTA-like complexes.

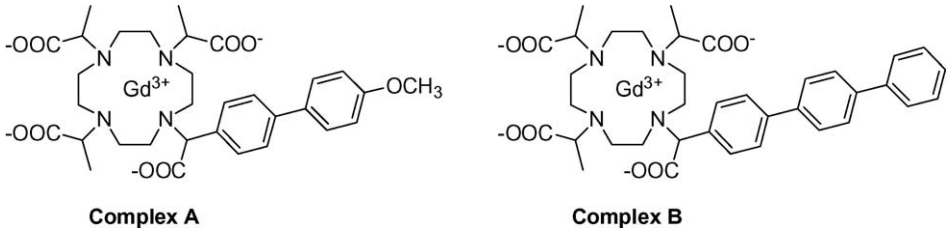

Fig. 7. Structure of two DOTMA-like derivatives bearing hydrophobic substituents for HSA binding.

not affect the coordination cage maintaining a fast exchange of the coordinated water. Both A and B complexes bind strongly to HSA yielding K_a values of 2.7×10^3 and $9.5 \times 10^4\ M^{-1}$, respectively. r_1^b of the complex A/HSA adduct, at 298 K and 20 MHz, is equal to $35\ mM^{-1}\ s^{-1}$. ^{17}O-measurements showed no difference between solutions containing the paramagnetic adduct and HSA alone. Clearly, the expected relaxation enhancement has been "quenched" by a direct interference of the donor groups on the surface of the protein with the inner hydration sphere of the Gd(III) ion. We could not determine whether it results in a replacement of the inner sphere water or simply in a dramatic elongation of its exchange lifetime. Thus, the biphenyl moiety does not appear long enough to protrude the chelate moiety outside the interference of the residues on the surface of the protein in proximity of the binding site. However, it is worth to note that the observed relaxation enhancement has to be ascribed to second sphere water molecules and mobile protons on the surface of the protein in the proximity of the paramagnetic center.

Complex B contains a binding synthon made up of three phenyl groups and resulted long enough to avoid such interference. Unfortunately, the low solubility of the adduct prevented the acquisition of ^{17}O NMR VT spectra, but we got an indirect assessment of the occurrence of the fast exchange of the coordinated water by measuring the water proton relaxation rates as a function of temperature. However, the observed r_1^b for B/HSA adduct is only $43.5\ mM^{-1}\ s^{-1}$, whereas the theory predicts much higher values for a system tumbling with the τ_R of HSA (30 ns) and the τ_M value of Gd-DOTMA.

We surmise that the "quenching" of the relaxation enhancement has to be associated to a molecular reorientational correlation time, for the coordinated water, that is significantly shorter than that one of the macromolecule. This would not depend on a wide-amplitude internal motion of the chelate as the binding through the terphenyl substituent is tight enough to hinder the rotation of the hydrophobic substituent inside the protein pocket. Rather the observed behaviour would be related to an internal rotation of the coordinated water along its coordination axis which overlaps with the overall motion of the macromolecular adduct.

Recently, Caravan and co-workers [27] tackled the problem of the residual mobility of a Gd(III) complex bound to HSA by designing a system containing two anchoring sites on the protein. Interestingly, the observed relaxivity for such adduct, though high ($60\ mM^{-1}\ s^{-1}$), is still significantly lower than that foreseen by the paramagnetic relaxation theory.

On our side, a derivative of Gd-AAZTA containing a long aliphatic chain (Gd-AAZTA-C17) has been synthesized and its relaxometric properties investigated in detail (manuscript in preparation). The complex showed to have the outstanding properties of the parent complex, namely: (i) two inner sphere water molecules in fast exchange with the bulk; (ii) high thermodynamic stability in aqueous solution; (iii) a nearly complete inertness towards the influence of bidentate endogenous anions. The functionalization with the hydrophobic chain induces the formation of micelles, with a relaxivity of $30\ mM^{-1}\ s^{-1}$ at 20 MHz and 298 K, already at sub-millimolar concentrations (cmc 0.1 mM). At concentration lower than cmc Gd-AATZA-C17 displays a high affinity binding to human serum albumin $K_a = 2.4 \times 10^4\ M^{-1}$ giving a macromolecular adduct endowed with the higher relaxivity value ($84\ mM^{-1}\ s^{-1}$) to now reported for HSA bound Gd-complexes.

2.2. Responsive agents

The term "responsive" refers to diagnostic agents whose contrasting properties are sensitive to a given physico-chemical variable that characterizes the microenvironment in which the probe distributes. Typical parameters of primary diagnostic relevance include pH, temperature, P_{O_2}, enzymatic activity, redox potential and concentration of specific ions and low-weight metabolites.

Unfortunately, their clinical use is still uncertain mainly because an accurate measurement of one of the above-mentioned parameters with a given relaxing probe requires a precise knowledge of the local concentration of the contrast medium in the region of interest. Only if the actual concentration is known, the observed change in the relaxation rate of water protons can be safely attributed to a change of the parameter to be measured.

2.2.1. pH sensitive

The design of a Gd(III) based complex whose relaxivity is pH-dependent requires that at least one of the structural or dynamic parameters determining its relaxivity is made pH-dependent. In most of the examples so far reported the pH dependence of the relaxivity reflects changes in the hydration of the metal complex.

For instance, we found that the relaxivity of a series of macrocyclic Gd(III) complexes bearing β-arylsulfonamide groups is markedly pH-dependent (Fig. 8) on passing from about $8\ s^{-1}\ mM^{-1}$ at pH < 4 to ca. $2.2\ s^{-1}\ mM^{-1}$ at pH > 8 [28]. It has been demonstrated that the observed decrease (about four-fold) of r_1 is the result of a switch in the number of water molecules coordinated to the Gd(III) ion from 2 (at low pH values) to 0 (at basic pHs). This corresponds to a change in the coordination ability of the β-arylsulfonamide arm that binds the metal ion only when it is in the deprotonated form.

In some cases, the pH dependence of the relaxivity is associated with changes in the structure of the second hydration shell. Two such systems have been reported by Sherry's group. The first case deals with a macrocyclic tetramide derivative of DOTA (DOTA-4AmP) that possess an unusual r_1 versus pH dependence [29]. The relaxivity of this complex increases from pH 4 to 6, decreases up to pH 8.5, remains constant up to pH 10.5 and, then, increases again. The authors suggested that this behaviour is related to the formation/disruption of the hydrogen bond network between the pendant phosphonate groups and the water bound to the Gd(III) ion. The deprotonation of phosphonate occurring at pH > 4 promotes the formation of the hydrogen bond network that slows down the exchange of the metal bound water protons. On the contrary, the behaviour observed at pH > 10.5 was accounted for in terms of a shortening of τ_M catalysed by OH^- ions. Recently, it has been demonstrated that this complex can be successfully used "in vivo" for mapping renal and systemic pH [30].

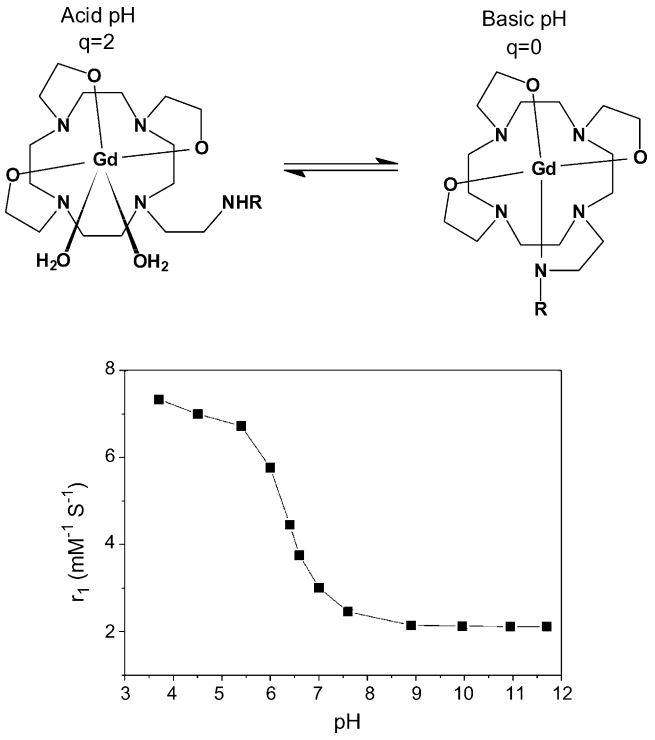

Fig. 8. pH dependence of the relaxivity (20 MHz, 25 °C) of a Gd(III) complex bearing an arylsulfonamide group. The protonation/deprotonation process of the arylsulfonamide group determines a variation in the hydration of the complex.

pH-dependent probes can also be obtained when the proton concentration is able to affect the structure of a macromolecular substrate that, in turn, results in changes of its dynamic properties. An interesting example is represented by a macromolecular Gd(III) construct formed by 30 Gd(III) units covalently linked, by a squaric acid moiety, to a poly-ornithine (114 residues; Fig. 9) [31].

At acidic pH the unreacted amino groups of the polymer are protonated and, therefore, tend to be localized as far as possible, whereas at basic pH the progressive deprotonation of the NH_3^+ groups determines an overall rigidification of the polymer structure owing to the formation of intramolecular hydrogen bonds between adjacent peptidic linkages. As expected, the reduced rotational mobility of the polymeric backbone upon increasing pH enhances the relaxivity of the system. Nevertheless, even if the enhancement is not particularly remarkable (ca. 40% in the 3–8 pH interval), it is worth to note that the relaxivity of this system is considerably higher than the previous examples over the entire pH range, thus allowing, in principle, the detection of pH changes at lower concentration of the responsive probe.

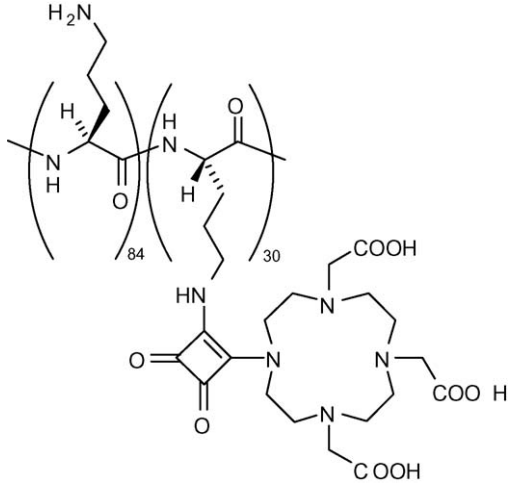

Fig. 9. Schematic representation of the macromolecular construct formed by ca. 30 Gd(III) units covalently linked, by a squaric acid moiety, to a poly-ornithine.

2.2.2. Agents sensitive to the redox potential

A diagnostic MRI probe sensitive to the in vivo redox potential would be very useful for detecting regions with a reduced oxygen partial pressure (P_{O_2}), in several pathologies including strokes.

Very few Gd(III) chelates sensitive to the tissue oxygenation have been so far reported. Our group has investigated the potential ability of GdDOTP to act as an allosteric effector of hemoglobin [32]. In fact, it has been observed that this chelate binds specifically to the T-form of the protein that is characterized by a lower affinity towards oxygen. The interaction is driven by electrostatic forces and leads to a significant relaxivity enhancement (ca. five-fold) owing to the restricted molecular tumbling of the paramagnetic complex once it is bound to the protein. Although hemoglobin can be considered as an excellent indirect target for detecting P_{O_2}, the practical applicability of the method suffers for the inability of GdDOTP to enter red blood cells.

Another approach deals with the use of liposomes built up with an amphiphilic Gd(III) complex containing a radical-sensitive disulfide bridge [33]. The relaxivity (at 20 MHz and 25 °C) of the liposomal paramagnetic agent is 13.6 s^{-1} mM^{-1}, i.e. two-fold higher than the free Gd(III) complex (r_1 of 6.5 s^{-1} mM^{-1}). Likely, the limited relaxivity enhancement is due to the rotational flexibility of the complex bound to the liposome. This system was tested "in vitro" by inducing the cleavage of the S–S bond chemically (by dithiothreitol) or physically (by γ-rays). In both cases, the relaxivity decreased from the value of the liposomal agents to that one of the free Gd(III) complex.

2.2.3. Enzyme responsive

One possible route to design enzyme responsive agents is to synthesise paramagnetic inhibitors, whose binding to the active site of the protein can be signalled by the consequent relaxivity enhancement. An example of this approach has been provided by Anelli et al., who synthesised a linear Gd(III) complex bearing an arylsulfonamide moiety (Fig. 10), that is a well-known inhibitor of carbonic anhydrase [34].

In vitro experiments demonstrated that this complex binds quite strongly (K_a of about 1.5×10^4) to the enzyme and its relaxivity in the bound form being about five-fold higher than the free complex (27 s^{-1} mM^{-1} versus 5 s^{-1} mM^{-1} at 20 MHz). Unfortunately, an attempt to test the validity of this "in vivo" approach failed, likely owing to the small amount of enzyme circulating in the blood.

An alternative approach is to design Gd(III) complexes acting as substrate for a specific enzyme. Along this direction, an exam-

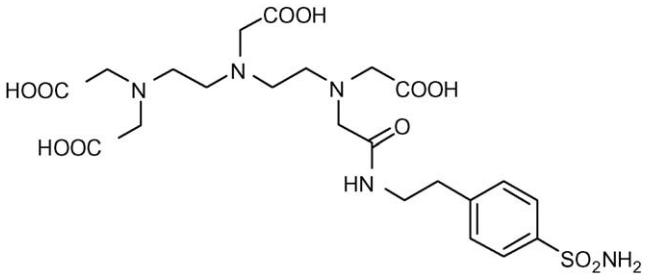

Fig. 10. Schematic representation of a ligand bearing an arylsulfonamide moiety whose Gd(III) complex shows a high binding affinity towards carbonic anhydrase.

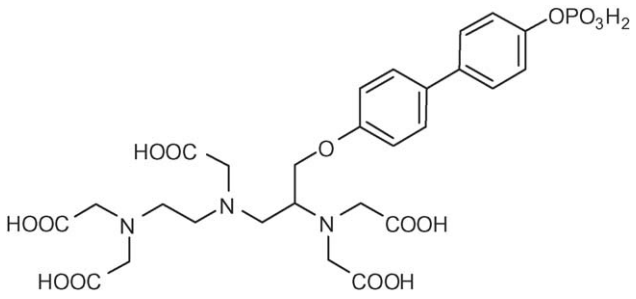

Fig. 11. Schematic representation of a ligand containing a phosphoric ester whose Gd(III) complex is responsive to serun alkaline phosphatase.

ple has been provided by Lauffer et al. who prepared a Gd(III) chelate containing a phosphoric ester sensitive to the attack of the serum alkaline phosphatase (Fig. 11) [35]. The hydrolysis yields the exposure of an hydrophobic moiety well suitable to bind to HSA. Upon binding, there is an increase of the relaxivity as a consequence of the lengthening of the molecular reorientational time. This approach was used by the same research group for designing Gd(III) complexes sensitive to thrombin-activatable fibrinolysis inhibitor (TAFI), a carboxypeptidase B involved in the clot degradation [36].

3. Cell labeling with Gd(III) chelates

The rapidly growing field of cellular therapy requires the development of efficient procedures for cell tracking in vivo. MRI can do it if the administered cells have been suitably labeled with magnetically active agents. In addition to the use of iron oxide particles, we and others have shown that cellular labeling can be successfully carried out with Gd(III) chelates. Two routes have been explored for pursuing an efficient entrapment of Gd(III) chelates in cells incubated in culture media: (i) via pinocytosis and (ii) via phagocytosis.

3.1. Pinocytosis

The cell internalized portion of the surrounding fluid by means of the invagination of its membrane and formation of small vesicles ($\leq$150 nm diameter) called endosomes. Therefore, incubation of cells for a sufficiently long time, in a medium containing the imaging probe at relatively high concentration leads to its internalization at amounts that may be sufficient for MRI visualization. Among a number of systems we have considered the neutral, highly hydrophilic Gd-HPDO3A that appears to be a good candidate for labeling stem cells by the pinocytotic route [37]. The in vivo MR visualization of labeled stem cells will allow their monitoring after transplantation. In a typical experiment of uptake via pinocytosis, few millions of stem cells are incubated in a culture medium containing Gd-HPDO3A in mM concentration range (10–50 mM) for few hours. Upon incubation, no saturation effect is observed and the amount of uptaken Gd is linearly proportional to the concentration of the paramagnetic agent in the incubation medium. Once cell internalized, the Gd-HPDO3A molecules result entrapped in endosomic vesicles as it can be checked out by observing the cells incubated with Eu-HPDO3A at the confocal microscope. In fact, Gd and Eu chelates with the same ligands display the same chemical/biological behaviour and the fluorescent response of Eu-HPDO3A acts as a histological reporter of the localization of Gd-HPDO3A in the cell. We have proved the potential of this approach by observing a mouse model of angiogenesis, on which blood-derived endothelial progenitor cells (EPCs) have been implanted subcutaneously, within a matrigel plug. After few days, the histological examination showed large capillary structure transposing the gel plugs. MR images parallel histological findings as hyperintense spots corresponding to the labeled cells were clearly detected. In Fig. 12, we report a MR image taken 14 days after implantation. As control, matrigel embed-

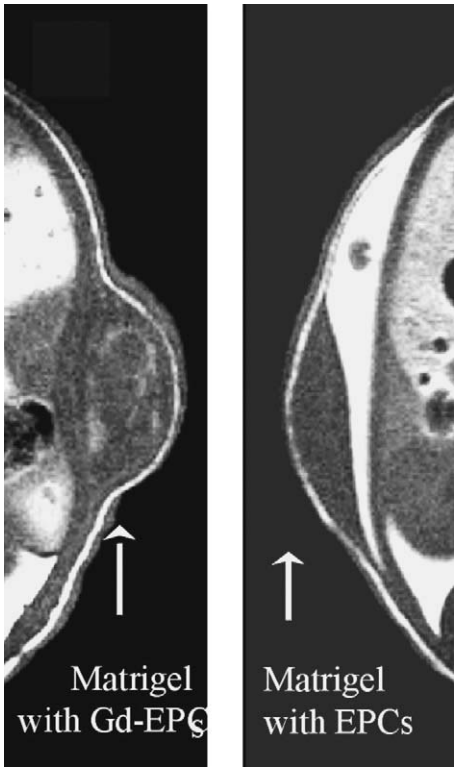

Fig. 12. In vivo T_1 weighted spin echo MR image (7.05 T) of EPCs labeled with Gd-HPDO3A (on the left). The cells are dispersed into a subcutaneous matrigel plug 7 days after the implantation. On the right, it is shown the control image of the same in the absence of the paramagnetic label.

ding unlabeled cells implanted in the same conditions are always negative for MRI signal.

This labeling procedure appears of general applicability. We have tested it on several tumor cell lines obtaining invariantly a very efficient uptake with no apparent cytotoxicity. Likely, the entrapment of Gd-HPDO3A into the endosomic vesicles prevents any impact of the paramagnetic agent on relevant cellular process meanwhile maintaining the full accessibility to cytoplasmatic water molecules.

3.2. Phagocytosis

It is the process of internalization of particles by cells endowed with phagocytic activity. In such a case, this route appears highly efficient for a single step internalization of a large amount of imaging probes. However, to be effective on MR images, Gd chelates must be water-soluble. Therefore, the particles must be biodegradable in order to release soluble Gd chelates once internalized into phagocytic cells. One may envisage several ways for the release of the Gd chelates. For instance, one may think of gel nano-particles of chitosan loaded with negatively charged Gd chelates. Such particles (200–400 nm diameter) are easily phagocyted and slowly degraded once internalized into the cells. Another approach to biodegradable Gd-containing particles has been pursued by designing particles whose insolubility is a property of the Gd chelates themselves [38]. This goal is easily reached by introducing long aliphatic chains on the surface of the ligand. However, one can control the fate of these systems by means of the functionality used to link the insolubilizing moiety to the Gd chelate. In fact, by using ester or peptidic functionalities, the insolubilizing synthon can be displaced from the Gd chelates by the activity of the proper enzyme (Fig. 13).

4. Targeting cells with suitably functionalized Gd(III) based probes

Targeting of contrast agents to specific epitopes on cellular membranes is a subject of increasing attention in the context of new directions of medical imaging represented by molecular imaging that aims at the in vivo visualization of molecular events occurring at cellular level. The development of approaches that visualize molecules that are the "signature" of a given disease represents a paradigm shift from the diagnostic modalities currently available in the clinic.

The basis for designing imaging probes for a given application is dictated by the localization profile of the target molecule (vascular, extracellular matrix, cell membrane, intracellular, near or at the cell nucleus). The development of high affinity ligands and their conjugation to the contrast agent is one of the key-steps for pursuing efficient molecular imaging probes. MRI-Gd(III) based agents are much less sensitive than radionuclear and optical imaging probes. Therefore, molecular imaging based on MRI, invariantly involves the need of accumulating a high number of contrast enhancing units at the site of interest.

The most accessible targets are those present on the surface of endothelial vessels. In principle they can be visualized by a number of macromolecular conjugates containing many Gd(III) complexes endowed with the proper vector recognizing the given target. Some years ago, a nice example of targeting an endothelial site was reported by Sipkins et al. [39] in the targeting of a specific angiogenesis marker, the endothelial integrin $\alpha_v\beta_3$, whose presence has been shown to correlate with tumor grade. The imaging probe used in this work is a Gd-containing polymerized liposome. The target is first bound by a biotinilated antibody against $\alpha_v\beta_3$, which is successfully recognized by an

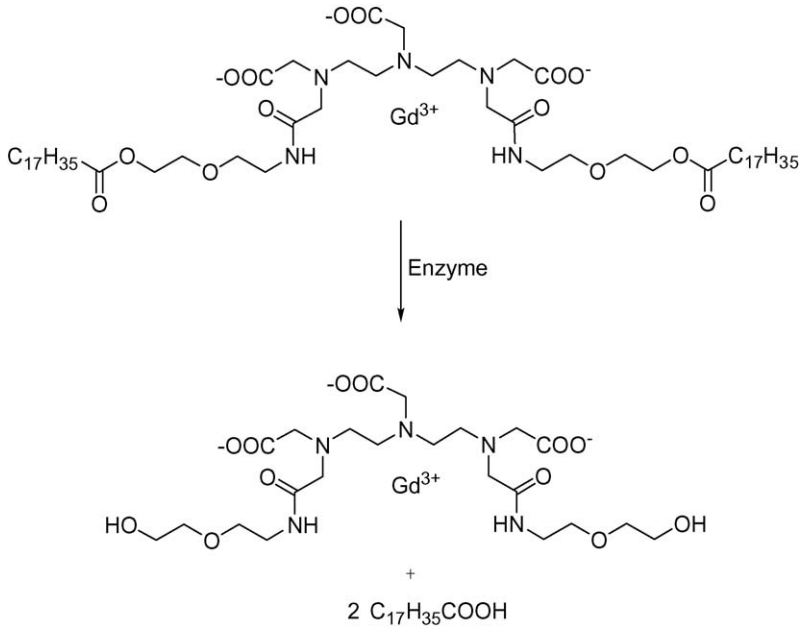

Fig. 13. The insoluble system is represented by a Gd-DTPA-like complex functionalized with a long aliphatic chain which is bound to the chelate moiety through an ester bond. The solubilization is obtained through the enzymatic cleavage of the ester bonds yielding to a soluble Gd(III) complex.

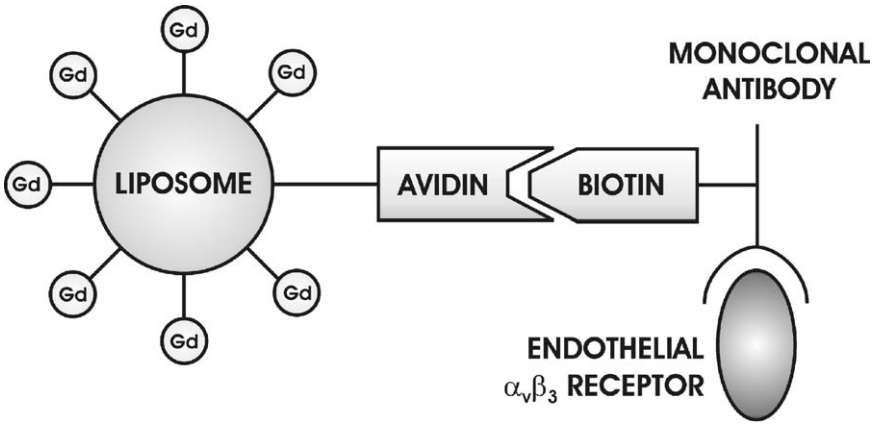

Fig. 14. Targeting of the endothelial integrin $\alpha_v\beta_3$ as a specific angiogenesis marker. The receptor is recognized by a biotinylated antibody that is then bound by an avidin moiety bearing a Gd(III) loaded liposome.

avidin moiety on the surface of the liposome. Each liposome as a mean diameter of 300–350 nm, which appears suitable to avoid the uptake by the reticuloendothelial system (Fig. 14). This approach provided enhanced and detailed detection of rabbit carcinoma through the imaging of the angiogenetic vasculature. Recently, the same $\alpha_v\beta_3$ target has been addressed with lipidic nano-particles containing a huge number of Gd chelated units (94,400 Gd/particle characterized by $r_1 = 19.1\ s^{-1}\ mM^{-1}$ (per Gd) = 1,800,000 per particle). One of the lipidic components is covalently bound to the $\alpha_v\beta_3$ integrin peptidomimetic antagonist [40].

The large molecular size of these constructs limits their delivery to targets on the endothelial walls. To target receptors in solid tissues other routes have to be followed. Bhujwalla et al. [41] have recently developed and applied a two-component Gd-based avidin–biotin system for the visualization of HER-2/scan receptors. The latter is a member of the epidermal growth factor family and it is amplified in multiple cancers. Their approach consisted of addressing the extracellular domain of the receptors by means of a biotinilated mAb. After clearance of the unbound mAb, Gd-labeled avidin is administered and binds, with high affinity, to the biotinilated mAb. The expression level of the receptor was estimated at 7×10^5 receptors/cell and the average number of Gd-DTPA units per avidin molecule was 12.5. The method has been successfully applied in an experimental mouse model of breast carcinoma.

We have investigated in detail the MR-imaging properties of the ternary adducts formed by multi-layered biotin/avidin/Gd(III) complexes. The most straightforward route is represented by the use of biotinilated agents such as those reported in Fig. 15. The bis-biotinilated derivative promotes the formation of systems made up by several layers of protein/complex adduct and it is therefore useful for the accumulation of the paramagnetic complex at the site of interest. As far as the efficiency of T_1-relaxing agent is concerned, the Gd-bis-biotinilated DTPA reported in Fig. 15 has the drawback of the limited enhancement upon the formation of the macromolecular adduct. In fact, it is well established that bis-amide DTPA complexes of Gd(III) possess sufficiently long exchange lifetime of the coordinated water which "quenches" the effect associated to the short T_{1M} values of water protons of paramagnetic macromolecular complexes. The relaxivity (r_1) of Gd-bis-biotinilated DTPA is 6.3 $mM^{-1}\ s^{-1}$ which increase to 9.2 $mM^{-1}\ s^{-1}$ in the 1:1 adduct with avidin and then further to 15.7 $mM^{-1}\ s^{-1}$ for the largest adduct.

When the bis-amide complex is replaced by a mono-biotinilated Gd-DTPA complex, whose τ_M is significantly shorter than that of the bis-biotinilated derivative, the relaxivity of the 1:1 adduct with avidin is significantly higher (r_{1p}^b = 25 $mM^{-1}\ s^{-1}$) than the corresponding adduct with the bis-amide derivative. Of course the use of the monobiotinilated Gd(Bio-LysDTPA) does not allow the formation of the layered structures peculiar of substrates containing two biotin moieties.

As biotinilated Ab (or FAb) are easily available, one may envisage the targeting of receptors on cell membranes through a three-step procedure: (i) first, the administration of the biotinilated Ab followed by (ii) the supply of avidin and then (iii) the Gd complex functionalized with the biotin moiety. In the case of bis-biotinilated Gd(III) complexes, steps (ii) and (iii) can be repeated several times.

4.1. Gd-loaded apoferritin

Cell-internalization via receptors is the route of choice in a number of nuclear medicine assays. For MRI, the design of the imaging probe requires the attachment of one or more Gd(III)-chelates to the ligand molecule. Such structural modification may drastically affect the internalization process in respect to the mechanism occurring for the native ligand.

In order to deal with a system whose structural characteristics were unaltered by the loading with Gd(III) chelates, we choosed apoferritin because it allows the imaging probes to be entrapped inside its inner cavity (Fig. 16) [42]. In apoferritin, the cavity has a diameter of 7–8 nm and an overall volume that can accomodate several small-sized Gd(III) complexes. The entrapment of ca. 10 Gd-HPDO3A molecules inside the apoferritin cavity has been carried out. In such a system, water can freely diffuse through the channels formed at intersection of the protein subunits, but not Gd-HPDO3A molecules (whose diameter is ca. 8–9 Å). The relaxivity shown by each Gd(III) complexes entrapped in the apoferritin is very high (ca. 80 $mM^{-1}\ s^{-1}$ at 20 MHz and 298 K).

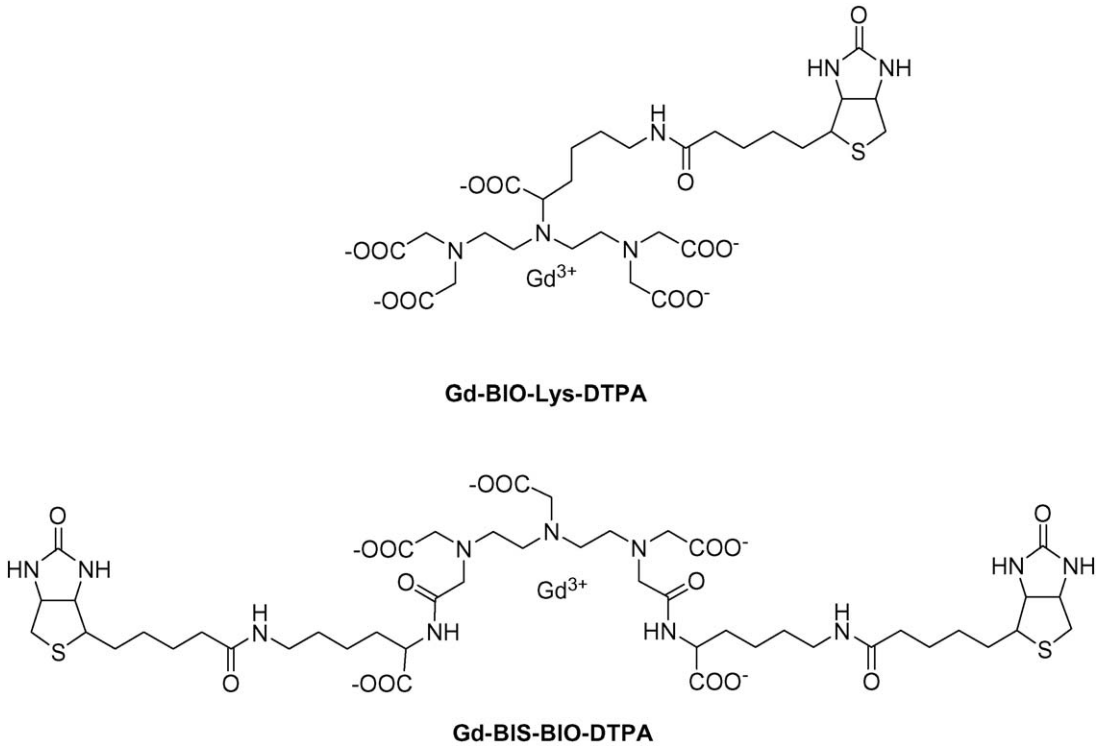

Fig. 15. Schematic representation of mono- and bis-biotinilated complexes (the bis-biotinilated one is a commercially available ligand).

This value is almost 20 times higher than the r_1 value of the free Gd-HPDO3A in water (4.2 mM^{-1} s^{-1}).

The $1/T_1$ nuclear magnetic relaxation dispersion (NMRD) profile recorded over 0.01–20 MHz frequency range shows that Gd-loaded apoferritin possesses a high relaxivity at any field with a further enhancement centered at 35 MHz, typical of slowly moving systems. Thus, the inclusion of several paramagnetic complexes in the apoferritin cavity allows multiple interaction pathways to be operative between the paramagnetic Gd(III) centers, the water molecules (freely moving within the cavity, or forming hydration layers on the protein surface) and exchangeable protons of chemical functionalities exposed in the inner cavity of the protein. The resulting relaxation scheme is analogous to that occurring upon the formation of protein/paramagnetic complex adducts but it is now highly amplified by having a closed spherical compartment.

The exterior of such Gd(III)-loaded apoferritin is exactly the same as in the parent ferritin and then, once administered intravenously, it is quickly cleared-up by the proper receptors on hepatocytes [43]. It has been possible to assess that the Gd-loaded apoferritin maintains its integrity upon the cell-internalization process as the relaxivity observed for the cytoplasmatic extract corresponds to that one of the intact system. Finally, the amount of cell internalized Gd-loaded apoferritin is similar to that reported for the native ferritin (6.5×10^6 molecules per cell in 6 h).

Once Gd-loaded apoferritin is administered to mice, it accumulates in the liver which then appears hyperintense in the MR images.

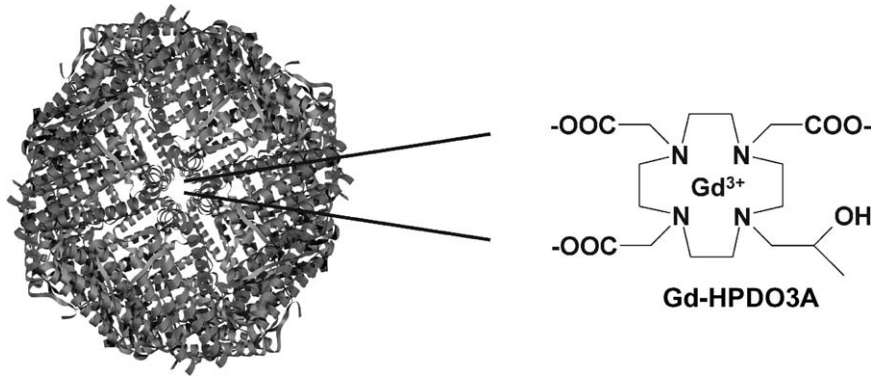

Fig. 16. Schematic representation of Gd-HPDO3A loaded apoferritin. About 10 Gd-HPDO3A complexes can be internalized in the inner cavity of the protein.

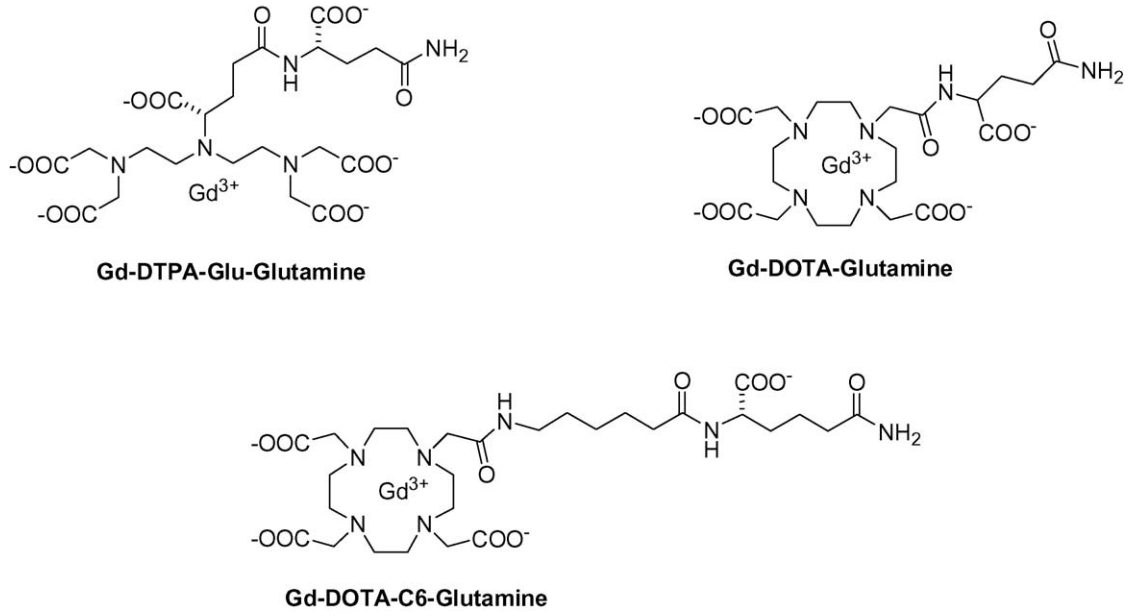

Fig. 17. Structures of Gd-DTPA and Gd-DOTA derivatives functionalized with glutamine residues.

4.2. Visualization of tumor cells via the amino acids transporting system

The amino acid transporter route appears an interesting one as such systems are intrinsically devoted to cell-internalization of large quantities of substrate molecules. In the field of CA for MRI examples of very efficient cellular uptake are already available. These examples rely essentially on hepatotropic agents represented by suitably functionalized Gd chelates. These systems enter the hepatocytes through transporting proteins, such as organic anion transport protein (OATP), which are present at high density on the cellular membrane [44]. Therefore, hepatotropic agents are particularly useful to assess the presence of secondary tumor lesions consisting of cells devoid of the efficient transporting system proper of hepatocytes.

Although a number of transporting systems may be considered, in the case of tumor cells, the transporters of choice appear those ones involved in the transport of nutrients and pseudo nutrients. In fact, during cell proliferation, the altered metabolism of tumor cells determines a much higher demand of these substances and therefore an increase of their uptake efficiency with up-regulation and/or overexpression of the corresponding membrane transporters [45–49].

We have tested whether this route allows to differentiate tumor from healthy cells by using a Gd-DTPA or DOTA chelate functionalized with a glutamine residue (Fig. 17). Glutamine is the most abundant amino acid in blood plasma and it is considered one of the most important nutrients for tumor cell metabolism [46–48]. Glutamine functionalized Gd-complexes have been added to the incubation media containing HTC and hepatocytes respectively. After few hours of incubation (Fig. 18), the amount of Gd chelate internalized in tumor cells is ca. four times higher than that uptaken by healthy hepatocytes. Furthermore, the involvement of glutamine transporters has been checked by adding glutamine in the medium containing the

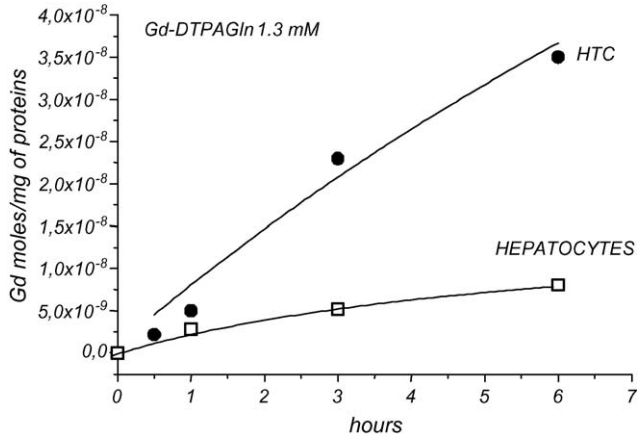

Fig. 18. Internalization of Gd-DTPA-glutamine into hepatocytes (□) and HTC cells (●). The uptake was carried out at 37 °C for 6 h.

glutamine-functionalized complexes. The amount of internalized Gd chelate decreases significantly upon increasing the amount of free amino acid in the incubation medium. Studies are in progress to assess whether the targeting of transporters with substrates containing Gd chelates moieties involves the formation of endosomic vesicles as well as to elucidate the metabolic fate of the internalized substances. Clearly, the possibility of targeting cells with low molecular weight, easy to synthesize, stable Gd chelates is highly attractive.

5. Chemical exchange saturation transfer (CEST) agents

Some years ago, a novel class of MRI contrast media, the so-called chemical exchange saturation transfer agents has been proposed [50]. Since then, the interest towards such agents has steadily grown, as witnessed by the increasing number of scien-

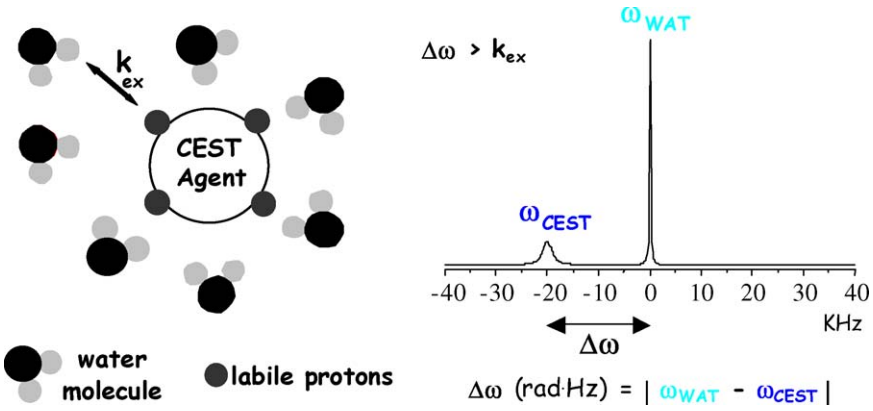

Scheme 1.

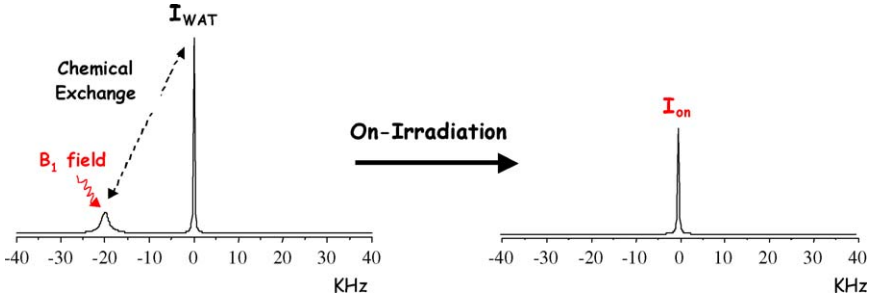

Scheme 2.

tific papers published each year on this subject. Their peculiar mechanism for generating contrast in an MR image makes these agents particularly attractive in respect to the conventional systems acting on the relaxation enhancement of water protons.

Basically, a CEST agent is a molecule containing labile protons, whose exchange rate with the bulk water protons is smaller than the separation of their resonance frequencies (expressed in rad Hz) (Scheme 1). When this condition is fulfilled, the resonance of the mobile protons of the CEST agent may be selectively saturated by using a specific radio frequency field of intensity B_1 (on-irradiation experiment; Scheme 2). The chemical exchange process transfers the saturated magnetization from the labile protons of the agent to the bulk water signal, whose intensity will then decrease accordingly. If this experiment is performed on a MRI scanner, the decreased signal intensity will result in the generation of a negative contrast (Fig. 19, panel B).

Unfortunately, the on-irradiation experiment is not sufficient for assessing the saturation transfer efficiency of a CEST agent. In fact, the saturation field may affect the intensity of the bulk water protons, even in the absence of the contrast medium because: (i) the saturation field may excite, and consequently saturate, directly the bulk water signal (and this phenomenon will be particularly relevant when the irradiation frequency is approaching the bulk water resonance) and (ii) in vivo, the irradiation field may saturate the extremely broad signal (up to 100 kHz) corresponding to the endogeneous mobile protons immobilised on the biological matrix (membranes, tissues, . . .). Fortunately, both these effects are only dependent upon the absolute value of the irradiated frequency; in other words, they are symmetric with respect to the resonance of the bulk water. On this basis, an accurate assessment of the saturation transfer efficiency of a CEST agent can be obtained by performing a second experiment (off-irradiation) in which the irradiating frequency is moved from the resonance of the mobile protons of the agent (e.g. −20 kHz in Scheme 2) to a new frequency defined by the same absolute value but with opposite sign (e.g. 20 kHz in Scheme 3).

It follows that the resulting water signal intensity I_{off} is somewhat lower than I_{wat} but it is higher than I_{on} in the presence of a

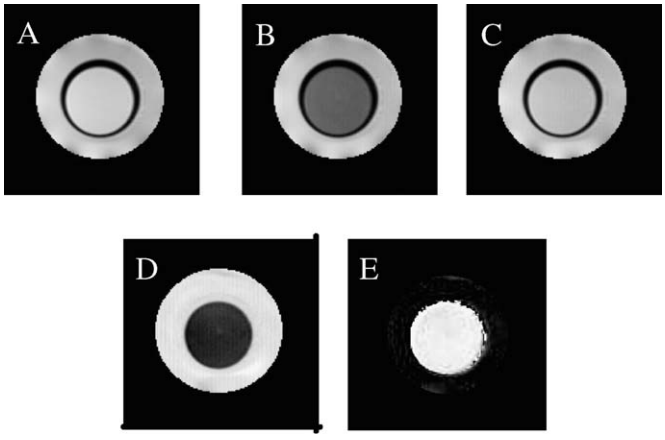

Fig. 19. Seven Tesla MR images of a phantom consisting of two coaxial tubes: the inner tube contains an aqueous solution of a PARACEST agent, whereas the outer tube contains neat water. (A) Proton density image (I_{inner} = 16.9 arbitrary units, a.u.); (B) on-irradiation CEST image (irradiation at −4800 Hz from bulk water, I_{inner} = 7.8 a.u.); (C) off-irradiation CEST image (irradiation at +4800 Hz from bulk water, I_{inner} = 14.5 a.u.); (D) on–off difference CEST image (ST% = 46.2); (E) ST_W image.

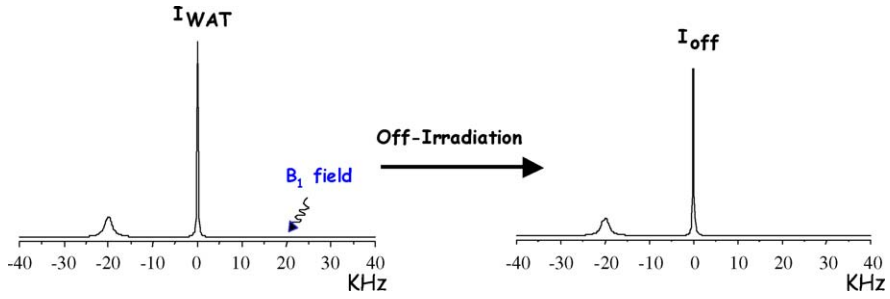

Scheme 3.

CEST agent (Fig. 19, panels B and C). Finally, the net saturation transfer (ST% expressed as percentage) due to the CEST agent can be simply calculated as: $ST\% = [1 - (I_{on}/I_{off})] \times 100$.

The ST contrast in a MR image can be visualized in two ways: (i) as difference between the on- and the off-MR experiments, in order to average out the regions in which there is no ST effect (Fig. 19, panel D) or (ii) as $ST_{weighted}$ map, in which the detection of the ST effect is visualized as an hyperintense spot whose brightness is reporter of the ST% parameter (Fig. 19, panel E). The advantage of the latter modality is that the ST effect, differently from the $(I_{on} - I_{off})$ entity, is not dependent upon the intensity of the water signal in the region of interest.

5.1. The sensitivity issue of CEST agents

On the basis of their mechanism of action, the CEST agents display the unique peculiarity of generating contrast only if the rf irradiation frequency corresponds to the absorption frequency of the mobile protons. It follows that the registration of a pre-administration image is not required because the visualization of the CEST agent is the result of the comparison between the on- and the off-resonance MRI scans and (ii) upon the co-administration of more CEST agents (with sufficiently different resonance frequencies of their mobile protons) one may detect their respective distribution in the same image [51]. As an extension of the latter concept, in the presence of different mobile protons belonging to the same agent (or to different agents characterized by the same pharmacokinetic properties), it is possible to produce images based on the ST effect which is not longer dependent on the concentration of the contrast medium but on a specific parameter that affects the rate of the magnetization transfer [52]. This feature can be properly exploited for designing novel MRI-CEST agents responsive to pH, temperature and metabolites concentration [53–55].

The most critical issue for the development of CEST agents is represented by their low sensitivity. Theoretically, the ST effect is dependent upon several parameters, among which, particularly relevant are k_{ex} and the number of mobile protons per molecule. The simulated curves reported in Fig. 20, calculated by using the theoretical model recently described by Woessner et al. [56], show the k_{ex} dependence of ST% at different B_1 field intensities. For a given set of parameters ($\Delta\omega$, T_1 and T_2 for the exchanging proton sites, concentration of mobile protons, magnetic field strength and irradiation time), the increase of k_{ex} leads to a *ST* enhancement up to a specific k_{ex} value, after which the efficiency of the saturation transfer drops off. Such a decrease cannot be ascribed to the approaching of the coalescence condition, because, being $\Delta\omega$ the same for all simulations, it occurs at different k_{ex} values. Rather, it is the result of the reduced number of mobile spins effectively saturated by the B_1 field owing to the broadening of their resonance associated to the increase of k_{ex}. The simulated profiles suggest that k_{ex} cannot be increased at will and, furthermore, that high B_1 intensity are required for maximising the ST effect. It is important to recall here that the largest B_1 value for an in vivo MR scan is limited, for safety purposes, by the specific absorption rate (SAR) value. For this reason, the design of highly sensitive CEST agents has to be pursued by increasing the number of mobile protons.

Fig. 21 reports a theoretical curve describing the dependence of the ST effect on the concentration of the irradiated protons. By considering a ST detection threshold of about 10%, the required concentration of mobile protons is in the order of few mM. Of course, the corresponding minimum concentration of CEST agent is dependent upon the number of mobile protons present per molecule. Actually, the detection limit for small-sized CEST agent (containing less than 10 protons/molecule), like amino acids, heterocyclic compounds, sugars or paramagnetic metal complexes is in the mM range [50,53,55,57]. A significant sensitivity improvement was achieved by investigating the ST properties of macromolecular agents, both diamagnetic (polyaminoacids, dendrimers and RNA-like polymers) [58,59]

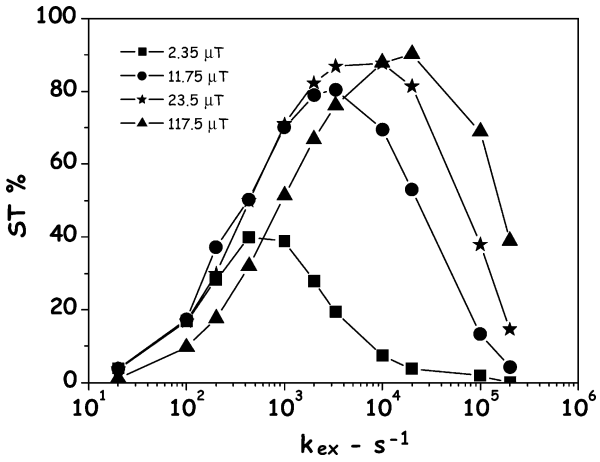

Fig. 20. Simulated k_{ex} dependence of ST% at different B_1 field intensity according to the theoretical model described in ref. [7]. (The data were calculated at 7 T, $\Delta\omega = 50$ ppm, concentration of mobile protons 50 mM, irradiation time 4 s.)

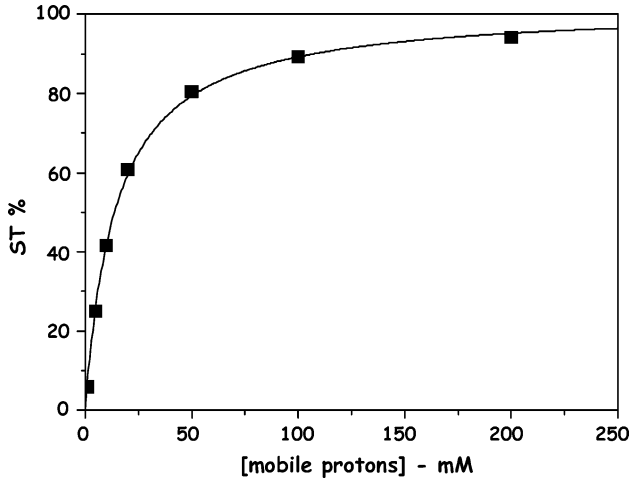

Fig. 21. Simulated dependence of ST% on the concentration of saturated mobile protons according to the theoretical model described in ref. [55]. (The data were calculated at 7 T, $\Delta\omega = 50$ ppm, $k_{ex} = 3300\ s^{-1}$, $B_1 = 11.75\ \mu T$, irradiation time 4 s.)

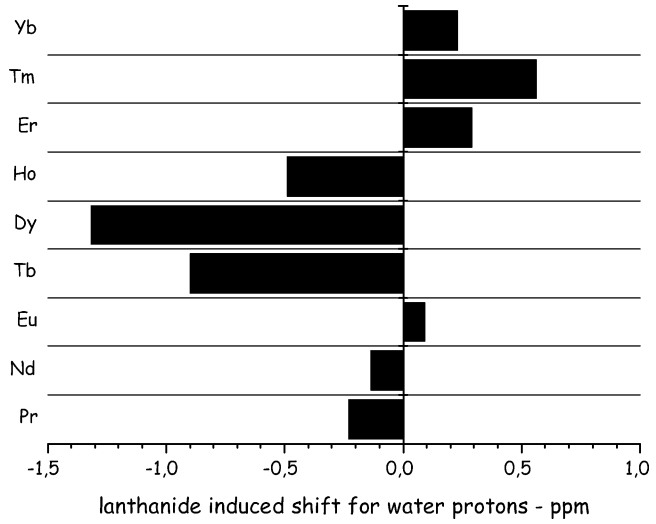

Fig. 22. Lanthanide induced shift for water protons measured at 14 T and 25 °C for 100 mM aqueous solution of $[Ln\text{-}DTPA]^{2-}$ complexes. The shifts refer to the resonance frequency of bulk water.

and paramagnetic ones [60]. Such systems contain thousands of mobile protons and, consequently, their detection limit is the μM range. Although the sensitivity displayed by the macromolecular CEST agents is close to the current limit for the clinical approved Gd(III) based agents, the possibility to exploit the peculiar properties of CEST media in molecular imaging MR protocols requires a further step forward.

5.2. LIPOCEST agents

A considerable sensitivity improvement can be achieved by considering nano-sized systems, which provide an extraordinarily large number of mobile protons. An optimal nano-system for developing highly-sensitive CEST agents is represented by liposomes, which are water-permeable lipidic vesicles widely used in pharmaceutical field primarily as drug delivery systems [61]. The number of mobile water protons which can be entrapped in a liposome cavity is in the range of 10^6–10^9 (for liposome diameters ranging from 50 to 400 nm), i.e. several order of magnitude higher than the values attainable for macromolecular agents. Furthermore, the water permeability of the liposome membrane may be varied by changing the formulation of the lipidic bilayer. For instance, it has been found that liposome membranes containing unsaturated phospholipids, like palmitoyl-oleyl-phosphatidyl choline (POPC), display higher water permeability than liposomes containing saturated lipids, like di-palmitoyl-phosphatidyl choline (DPPC) [62]. Furthermore, the water permeability can be further modified by adding cholesterol in the formulation. In order to be used for a CEST procedure, the resonance frequency of the water protons inside liposomes must be different with respect to the extraliposomial solvent. This requirement may be successfully accomplished by entrapping an hydrophilic paramagnetic shift reagent (SR) in the liposomial compartment. Lanthanide(III) complexes represent the most used and efficient class of shift reagents in aqueous solutions [63]. Fig. 22 reports the measured chemical shift values of water protons within the $[Ln\text{-}DTPA]^{2-}$ series, where all the complexes contain a fast-exchanging metal bound water molecule. In this isostructural series, the chemical shift of water protons is dominated by the dipolar interaction between ^{1}H-water nuclei and the unpaired electrons of the metal ion and, consequently, the observed shifts primarily reflects the paramagnetism of the metal center, which can be quantitatively expressed by the value of the Bleaney's constant [64]. On this basis, the most efficient Ln(III) ions are Dy(III) and Tm(III) causing upfield and downfield shifts, respectively. The paramagnetic lanthanide shift induced on water protons is also dependent on the ligand, as shown in Fig. 23, where the shifts of Dy- and Tm-DTPA are compared with those ones measured for some selected macrocyclic chelates of the same lanthanides.

On passing from the linear ligand DTPA to macrocyclic chelates, the shifting ability of the metal ions is considerably enhanced. In fact, the observed shifts are dependent on the cosine of the angle formed between the magnetic axes of the complex

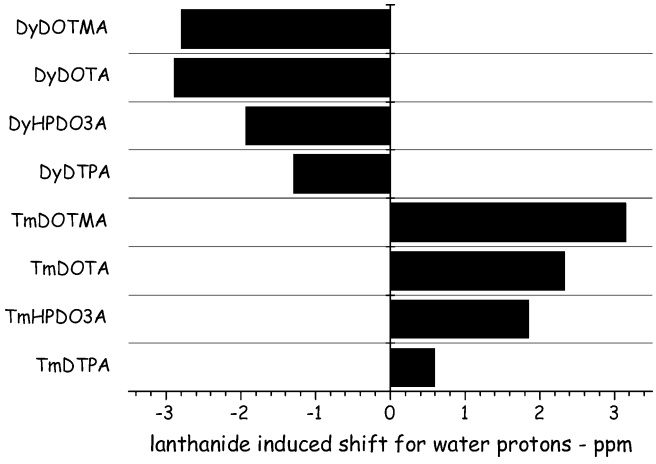

Fig. 23. Lanthanide induced shift for water protons measured at 14 T and 25 °C for 100 mM aqueous solution of the reported Ln(III) complexes. The shifts refer to the resonance frequency of bulk water.

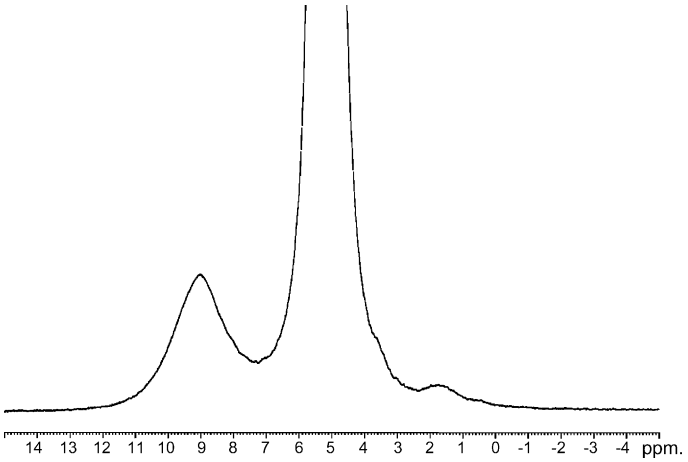

Fig. 24. ^{1}H NMR spectrum (14 T, 25 °C) of an aqueous suspension of a LIPOCEST preparation (SR = Tm-DOTMA, membrane composition: DPPC/DPPG 95/5, w/w). The resonance at ca. 9 ppm corresponds to the intraliposomal water protons downfield shifted by the paramagnetic shift reagent. The signal at ca. 1.8 ppm corresponds to the lipidic components of the liposome membrane.

and the proton-metal vector. In macrocyclic chelates, the metal-coordinated water molecule is much more aligned along the magnetic axes than in linear complexes and, consequently, the observed induced shifts are larger.

Liposomes entrapping a shift reagent for CEST purposes were called LIPOCEST agents [65] and Fig. 24 reports a typical ^{1}H NMR spectrum of a suspension of such nano-systems entrapping Tm-DOTMA as shift reagent. The peak at about 4 ppm downfield from the bulk water is assigned to the intraliposomal water protons, whereas the broad signal centered at about 1.8 ppm arises from the lipidic components of liposome membrane.

The sensitivity of LIPOCEST agents has been assessed by measuring the ST effect as a function of the liposome concentration. The result of this experiment is reported in Fig. 25, where two LIPOCEST agents, both entrapping similar amount of Tm-DOTMA, but differing in the formulation of the liposome membrane, are compared. The sensitivity of such systems, expressed by the concentration required for detecting a ST value of 10%, is very high, being in the sub-nanomolar range for both the tested agents. This result nicely parallels the increased number of mobile protons that, in these liposomes of about 240 nm of diameter, is of about five orders of magnitude larger than in a macromolecular agent. Furthermore, the sensitivity differences shown by the two LIPOCEST agents depend on the composition of their membranes. In fact, the increased water permeability due to the presence of an unsaturated fatty acid component (POPC) further enhances the sensitivity (<100 pM) of the corresponding LIPOCEST agent.

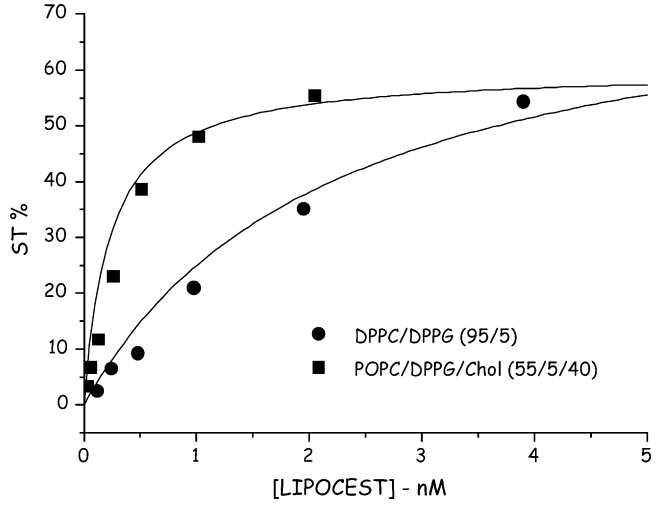

Fig. 25. ST% (7 T, 39 °C) as a function of the concentration of LIPOCEST agents for two preparations differing in the composition of the liposome membrane.

In summary, these very promising results suggest that LIPOCEST agents can be considered a real breakthrough in the field of MR agents based on saturation transfer. The sensitivity displayed by these agents is so high to foresee their use in molecular imaging protocols, where the peculiar properties of CEST systems (co-administration and MR detection of a mixture of agents) could substantially improve the diagnostic potential of MRI. Furthermore, though the use of nano-sized systems somehow limits the number of accessible targets, LIPOCEST agents can fully exploit the biodistribution properties of liposomes, e.g. their ability to be accumulated, both passively and actively, in solid tumors [66].

6. Conclusions

In the last two decades, the chemistry of lanthanide(III) chelates has been subject of an extraordinary interest for the potential use of these complexes as contrast agents for MRI investigations. This has led to the synthesis of a number of hepta- and octa-coordinating ligands able to wrap around the Ln(III) ions in order to yield chelates characterized by very high thermodynamic stabilities. Moreover, much attention has been devoted to relate the structure of Ln(III) chelates to the exchange rate of the coordinated water molecule(s). These studies have dramatically extended the range of available exchange rates, which now cover a range from few nanoseconds to several microseconds.

The acquisition of an in-depth knowledge of the structural electronic and dynamic determinants of the observed relaxivity has prompted interesting activities in the direction to make the latter parameter responsive to specific characteristics of the biological environment of the contrast agent. This may find unique applications in medical diagnosis.

The need to conjugate high relaxivity Gd(III) chelates to suitable synthons that deliver the contrast agent to the targeting sites has prompted innovative synthetic routes that allows an efficient coupling to a number of vectors including peptides, peptido-mimetics, lipids, sugars and proteins. Often it has been found more useful to design systems able to form highly stable supramolecular adducts with the macromolecule of interest.

Finally, the huge work on Gd(III) chelates has prompted new activities with other lanthanide(III) ions that has led to the development of the novel class of CEST agents. Their potential can be very high as it allows to exploit more contrast agents in the same MR-image as each of them will be activated “at will” by selecting the characteristic irradiation frequency.

Acknowledgements

Support from Bracco Imaging Spa, MIUR, Noe-EMIL and DiMI are gratefully acknowledged. This work was carried out under the frame of EU-Cost D18 and D32 Actions.

References

[1] I.R. Young, Methods in Biomedical Magnetic Resonance Imaging and Spectroscopy, John Wiley & Sons Ltd., Chichester, 2000.
[2] P.A. Rinck, Magnetic Resonance in Medicine, ABW Wissenschaftsverlag GmbH, Berlin, 2003.
[3] M.F. Tweedle, in: J.-C.G. Bünzli, G.R. Choppin (Eds.), Lanthanide Probes in Life, Chemical and Earth Sciences: Theory and Practice, Elsevier, Amsterdam, 1989, p. 127.
[4] E. Brücher, A.D. Sherry, in: A.E. Merbach, E. Tóth (Eds.), The Chemistry of Contrast Agents in Medical Magnetic Resonance Imaging, Wiley, Chichester, 2001, p. 243.
[5] H.J. Weinmann, A. Mühler, B. Radüchel, in: I.R. Young (Ed.), Biomedical Magnetic Resonance Imaging and Spectroscopy, John Wiley & Sons Ltd., Chichester, 2000, p. 705.
[6] P. Caravan, J.J. Ellison, T.J. McMurry, R.B. Lauffer, Chem. Rev. 99 (1999) 2293.
[7] H. Schmitt-Willich, M. Brehm, C.L.J. Evers, et al., Inorg. Chem. 38 (1999) 1134.
[8] F. Uggeri, S. Aime, P.L. Anelli, et al., Inorg. Chem. 34 (1995) 633.
[9] E.J. Rummeny, G. Marchal, Acta Radiol. 38 (1997) 626.
[10] A. Roch, R.N. Muller, P. Gillis, J. Chem. Phys. 110 (1999) 5403.
[11] J.M. Colet, C. Pierart, F. Seghi, I. Gabric, R.N. Muller, J. Magn. Reson. 134 (1998) 199.
[12] L. Banci, I. Bertini, C. Luchinat, Nuclear and Electronic Relaxation, VCH, Weinheim, 1991, p. 91.
[13] M. Botta, Eur. J. Inorg. Chem. 3 (2000) 399.
[14] S. Aime, M. Botta, M. Fasano, E. Terreno, Chem. Soc. Rev. 27 (1998) 19.
[15] S. Aime, E. Gianolio, E. Terreno, et al., J. Biol. Inorg. Chem. 5 (2000) 488.
[16] S. Hajela, M. Botta, S. Giraudo, et al., JACS 122 (2000) 11228.
[17] S. Aime, M. Botta, L. Frullano, et al., J. Med. Chem. 43 (2000) 4017.
[18] S. Aime, L. Calabi, C. Cavallotti, E. Gianolio, G.B. Giovenzana, P. Losi, A. Maiocchi, G. Palmisano, M. Sisti, Inorg. Chem. 43 (2004) 7588.
[19] J.B. Livramento, E. Toth, A. Sour, A. Borel, A.E. Merbach, R. Ruloff, Angew. Chem. Int. Ed. 44 (2005) 1480.
[20] D.A. Fulton, M. O'Halloran, D. Parker, K. Senanayake, M. Botta, S. Aime, Chem. Commun. 4 (2005) 474.
[21] S. Aime, M. Botta, M. Fasano, et al., in: A.E. Merbach, E. Toth (Eds.), The Chemistry of Contrast Agents in Medical Magnetic Resonance Imaging, John Wiley & Sons Ltd., Chichester, 2001, p. 193.
[22] R.B. Lauffer, D.J. Parmalee, et al., Radiology 207 (1998) 529.
[23] S. Aime, M. Chiaussa, G. Digilio, et al., J. Biol. Inorg. Chem. 4 (1999) 766.
[24] D.H. Powell, O.M. Ni Dhubhghaill, D. Pubanz, L. Helm, Y.S. Lebedev, W. Schlaepfer, A.E. Merbach, J. Am. Chem. Soc. 118 (1996) 9333.
[25] S. Aime, A. Barge, M. Botta, A.S. De Sousa, D. Parker, Angew. Chem. Int. Ed. 37 (2000) 2673.
[26] S. Aime, E. Gianolio, D. Longo, R. Pagliarin, C. Lovazzano, M. Sisti, Chemibiochem 6 (2005) 818.
[27] Z.D. Zhang, M.T. Greenfield, M. Spiller, T.J. McMurry, R.B. Lauffer, P. Caravan, Angew. Chem. Int. Ed. 44 (2005) 6766.
[28] M.P. Lowe, D. Parker, O. Reany, et al., J. Am. Chem. Soc. 123 (2001) 7601.
[29] S.R. Zhang, K.C. Wu, A.D. Sherry, Angew. Chem. Int. Ed. 38 (1999) 3192.
[30] N. Raghunand, C. Howison, A.D. Sherry, et al., Magn. Reson. Med. 49 (2003) 249.
[31] S. Aime, M. Botta, S. Geninatti, et al., Chem. Commun. (1999) 1577.
[32] S. Aime, P. Ascenzi, E. Comoglio, et al., J. Am. Chem. Soc. 117 (1995) 9365.
[33] C. Glogard, G. Stensrud, S. Aime, Magn. Reson. Chem. 41 (2003) 585.
[34] P.L. Anelli, I. Bertini, M. Fragai, et al., Eur. J. Inorg. Chem. (2000) 625.
[35] R.B. Lauffer, T.J. Mc Murry, S.O. Dunham, et al., PCT Int. Appl. WO9736619 (1997).
[36] A.L. Nivorozhkin, A.F. Kolodziej, P. Caravan, et al., Angew. Chem. Int. Ed. 40 (2001) 2903.
[37] S. Geninatti Crich, L. Biancone, V. Cantaluppi, G. Esposito, S. Russo, G. Camussi, S. Aime, Magn. Reson. Med. 51 (2004) 938.
[38] S. Aime, C. Cabella, S. Colombatto, S. Geninatti Crich, E. Gianolio, F. Maggioni, JMRI 16 (2002) 394.
[39] D.A. Sipkins, D.A. Cheresh, M.R. Kazemi, L.M. Nevin, M.D. Bednarski, K.C.P. Li, Nat. Med. 4 (1998) 623.
[40] P.M. Winter, S.D. Caruthers, A. Kassner, T.D. Harris, L.K. Chinen, J.S. Allen, E.K. Lacy, H.Y. Zhang, J.D. Robertson, S.A. Wickline, G.M. Lanza, Cancer Res. 63 (2003) 5838.
[41] Z.M. Bhujwalla, D. Artemov, N. Mori, R. Ravi, Cancer Res. 63 (2003) 2723.
[42] S. Aime, L. Frullano, S. Geninatti Crich, Angew. Chem. Int. Ed. 41 (2002) 1017.
[43] K. Osterloh, P. Aisen, Biochem. Biophys. Acta 1011 (1989) 40.
[44] M. Lewin, O. Clement, P. Belguise-Valladier, L. Tran, C.A. Cuenod, N. Siauve, G. Frija, Invest. Radiol. 36 (2001) 9.
[45] O. Yanagida, Y. Kanai, A. Chairoungdua, D.K. Kim, H. Segawa, T. Nii, S.H. Cha, H. Matsuo, J. Fukushima, Y. Fukasawa, Y. Tani, Y. Taketani, H. Uchino, J.Y. Kim, J. Inatomi, I. Okayasu, K. Miyamoto, E. Takeda, T. Goya, H. Endou, Biochim. Biophys. Acta 1514 (2001) 291.
[46] C.L. Collins, M. Wasa, W.W. Souba, S.F. Abcouwer, J. Cell. Phys. 176 (1998) 166.
[47] W. Wiley, M.D. Souba, Ann. Surg. 6 (1993) 715.
[48] J.D. Mc Givan, Biochem. J. 330 (1998) 255.
[49] N. Seiler, J.G. Delcros, J.P. Moulinoux, Int. J. Biochem. Cell. Biol. 28 (1996) 843.
[50] K.M. Ward, A.H. Aletras, R.S. Balaban, J. Magn. Reson. 143 (2000) 79.
[51] S. Aime, C. Carrera, D. Delli Castelli, S. Geninatti Crich, E. Terreno, Angew. Chem. Int. Ed. 44 (2005) 1813.
[52] K.M. Ward, R.S. Balaban, Magn. Reson. Med. 44 (2000) 799.
[53] S. Aime, A. Barge, D. Delli Castelli, F. Fedeli, A. Mortillaro, F.U. Nielsen, E. Terreno, Magn. Reson. Med. 47 (2002) 639.
[54] S. Aime, D. Delli Castelli, E. Terreno, Angew. Chem. Int. Ed. 41 (2002) 4334.
[55] E. Terreno, D. Delli Castelli, G. Cravotto, L. Milone, S. Aime, Invest. Radiol. 39 (2004) 235.
[56] D.E. Woessner, S. Zhang, M.E. Merritt, A.D. Sherry, Magn. Reson. Med. 53 (2005) 790.
[57] S. Zhang, L. Michaudet, S. Burgess, A.D. Sherry, Angew. Chem. Int. Ed. 41 (2002) 1919.
[58] N. Goffeney, J.W.M. Bulte, J. Duyn, L.H. Bryant Jr., P.C.M. van Zijl, J. Am. Chem. Soc. 123 (2001) 8628.
[59] K. Snoussi, J.W.M. Bulte, M. Gueron, P.C.M. van Zijl, Magn. Reson. Med. 49 (2003) 998.
[60] S. Aime, D. Delli Castelli, E. Terreno, Angew. Chem. Int. Ed. 42 (2003) 4527.
[61] V.P. Torchilin, V. Weissig (Eds.), Liposomes, Oxford University Press, Oxford, UK, 2003.
[62] S.L. Fossheim, A.K. Fahlvik, J. Klaveness, R.N. Muller, Magn. Reson. Imaging 17 (1999) 83.
[63] J.A. Peters, J. Huskens, D.J. Raber, Prog. Nucl. Magn. Reson. Spectrosc. 28 (1996) 283.
[64] C.F.G.C. Geraldes, C. Luchinat, in: A. Sigel, H. Sigel (Eds.), Metal Ions in Biological Systems, vol. 40, 2003, p. 513 (Chapter 14).
[65] S. Aime, D. Delli Castelli, E. Terreno, Angew. Chem. Int. Ed. 44 (2005) 5513.
[66] A. Gabizon, H. Shmeeda, A.T. Horowitz, S. Zalipsky, Adv. Drug Deliv. Rev. 56 (2004) 1177.